A neural network based feedback linearising controller for HVDC links

P.K. Dash *, Aurobinda Routray, Sukumar Mishra

Department of Electrical Engineering, R.E.C. Rourkela 769 008, India

Abstract

Feedback linearization has been used successfully to address some of the practical control problems. This paper introduces a practical control philosophy for a point to point HVDC link, based on the above principle. The basic DC link equation has been used to evaluate the firing angle for the rectifier. An Adaline has been trained to identify the parameters of the simplified system model prior to the application of this control. The simulation results presented in this paper prove the advantage of the proposed control scheme.

Keywords: Adaline; Feedback linearization; HVDC link

1. Introduction

The inherent non-linearity involved in an HVDC link operation makes it difficult to design appropriate controllers under different normal and abnormal situations. The rate of change of the DC link current is highly sensitive to the firing angles on either side, due to the non-linear relationship between them. This leads to severe oscillations in DC link current and voltage waveforms as soon as a fault is cleared or the link is energized. These excursions impose a great deal of constraints in designing the converter valves, circuit breakers, reactors and filter banks. Sometimes the high value of di/dt and dv/dt can damage the associated equipment, especially the thyristor valves.

Literature available in the DC adaptive control [1] is inconclusive of it's practical application under large signal conditions. Several authors propose gain scheduling controllers for HVDC links for these conditions. Recently Reeve et al. has tried a gain scheduling adaptive control strategy for HVDC links [2,3]. Hammad et al. has developed a coordinated control scheme based on optimal control strategy for parallel AC–DC systems.

In this paper a new simplified control strategy based on the feedback linearization approach has been developed [4]. Prior to the application of control the basic model has been identified by an adaptive linear combiner (adaline) [5]. This model has been used to derive the firing angle for the converter valves. In the end, the simulation carried out using an EMTDC package [6–10] demonstrates the superiority of the proposed controller.

2. HVDC system model

A two-pole point-to-point 6-pulse HVDC system has been simulated with the help of EMTDC package [11]. The filters and transformers on either side of the DC link and the transmission line are represented in detail. The system shown in Fig. 1 is divided into four subsystems:

2.1. Subsystem 1

The rectifier side subsystem consists of a constant voltage and constant frequency source behind an impedance that comprises inductance and resistance to represent a simplified AC system. The short circuit
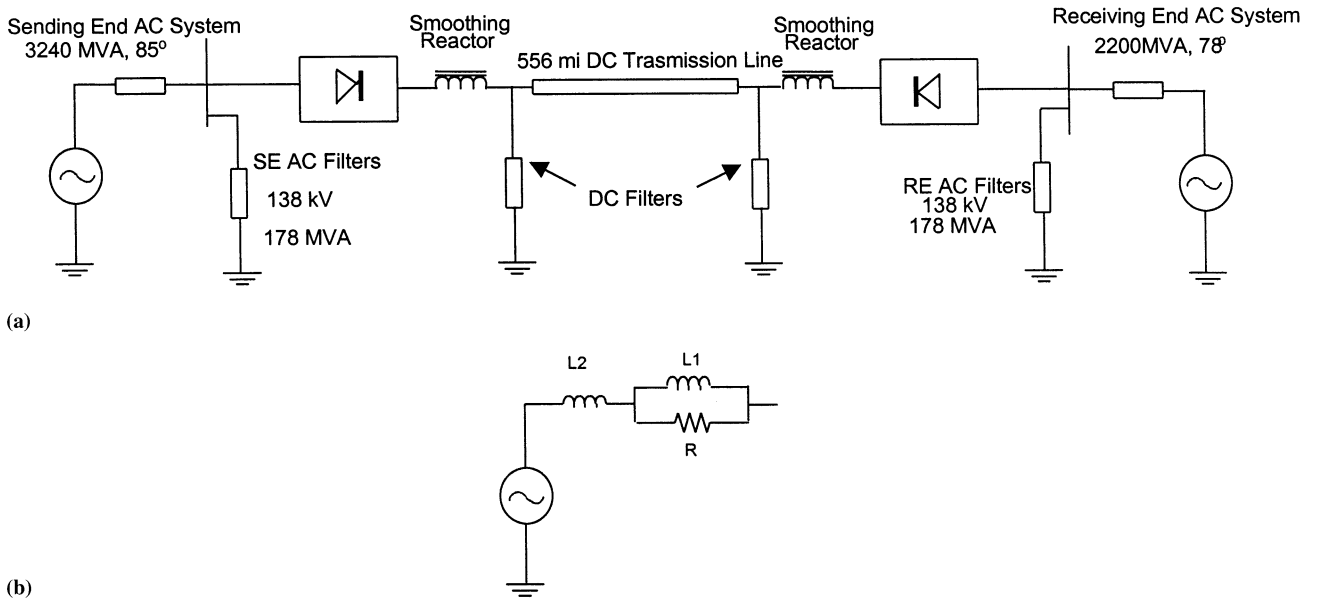
---

* Corresponding author.

Fig. 1. (a) HVDC System model. (b) Details of AC system representation.

ratio(SCR) for the system is fairly high (around 15) as compared to the Inverter side AC system. AC filters for 5, 7, 11 and 13th harmonics have been provided.

2.2. Subsystem 2

The rectifier is connected to the DC transmission line through a large inductor and a 6th harmonic filter has been connected to take care of the ripples in the DC voltage.

2.3. Subsystem 3

It is identical with the subsystem 2 except for the fact that it comes in-between the inverter and the DC link.

2.4. Subsystem 4

The inverter side AC system representation is identical to that of the rectifier side. The same filters are also present here, but the voltage ratings and SCR are different. The inverter end AC system is weaker having an SCR around 3.0.

2.5. Inverter control system

The inverter is in constant extinction angle (CEA) control (Fig. 2). The pole controller (i.e. current controller Fig. 3) also has been provided for rectifier operation under transient conditions. However, in steady state normal operating conditions it operates with CEA control. These are well documented controllers available in [11].

2.6. Rectifier control system

The DC-link current is maintained constant by subjecting the rectifier with feedback linearising constant current control (Fig. 4). The firing angle is adjusted with current error, to maintain the DC link current constant. It is also provided with a valve controller (Gamma controller) to operate it as an inverter during transient and abnormal situations.

3. Identification

During steady state the basic equation of a two terminal DC link is given by

$$\dot{I}_{dc} = \frac{V_{dor}}{L_{dc}} \cos\alpha_r + \frac{V_{doi}}{L_{dc}} \cos\alpha_i - \frac{R_{eq}}{L_{dc}} I_{dc} \qquad (1)$$

where,

$$R_{eq} = R_{cr} - R_{ci} + R_{dc}$$

R_{cr}, equivalent commutation reactance on the rectifier side; R_{ci}, equivalent commutation reactance on the inverter side; R_{dc}, DC link resistance.

In order to predict the changes in the dynamics of the ac systems (changes in their equivalent circuits) following an electrical disturbance on either of the ac systems connected to the dc link, the mathematical model of the HVDC system should include the Thevenin equivalents of both the ac systems. The values of R_{dc} and R_{ci} are obtained as [3].
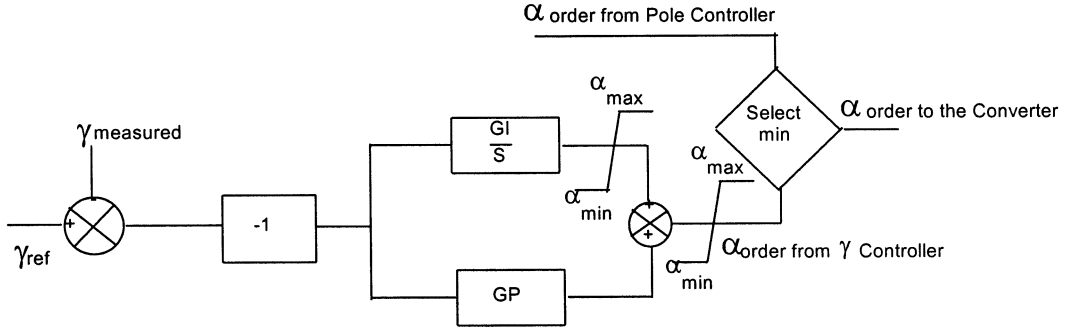
$$R_{cr} = \frac{6}{\pi} n^2 (X_t + l X_{thr})$$

Fig. 2. Inverter gamma controller.

and

$$R_{cr} = \frac{6}{\pi} n^2 (X_t + lX_{thi}) \tag{2}$$

where l is a proportionality factor developed in Ref. [3] and X_t is the reactance of the converter transformer, and n is converter transformer turns-ratio. X_{thr} and X_{thi} Thevenin equivalent reactance on the rectifier and inverter sides, respectively. Eq. (1) is rewritten as

$$\dot{I}_{dc} = K_1 \cos\alpha_r + K_2 \cos\alpha_i + K_3 I_{dc} \tag{3}$$

where K_1, K_2 and K_3 are functions of the voltages V_{dor}, V_{doi}, L_{dc} and R_{eq}.

Thus the HVDC system in Eq. (3) is of the form

$$\dot{x} = f(x) + g(x)u \tag{4}$$

with output $y = x$, the relative degree of the system is one,

$$f(x) = K_3 I_{dc} \tag{5}$$

and

$$g(x) = 1 \tag{6}$$

$$u = K_1 \cos\alpha_r + K_2 \cos\alpha_i \tag{7}$$

The HVDC link represented by Eq. (4) is fully linearisable as the relative degree and the order of the system are the same. Thus the interval dynamics or 'Zerodynamics' need not be considered [4].

Therefore, the feedback linearising control

$$u = \frac{1}{g(x)}(-f(x) + \vartheta) \tag{8}$$

applied to Eq. (4) results in the linear system

$$\dot{I}_{dc} = \vartheta \tag{9}$$

where ϑ can be chosen to result in a suitable performance of the system.

For the HVDC link, the rectifier firing angle α_r is found as

$$\alpha_r = \cos^{-1}\left(\frac{\vartheta}{K_1} - \frac{K_2 \cos\alpha_i - K_3 I_{dc}}{K_1}\right) \tag{10}$$

To find out ϑ, the following error tracking law is used to maintain I_{dc} constant.

The tracking error e is

$$e = I_{dcref} - I_{dc} \tag{11}$$

A tracking error equation of the form

$$\dot{e} + c_1 e + c_2 \int_0^t e\,dt = 0 \tag{12}$$

yields

$$\dot{e} = -\dot{I}_{dc} = -c_1 e - c_2 \int_0^t e\,dt = 0 \tag{13}$$

Hence

$$\vartheta = c_1 e + c_2 \int_0^t e\,dt \tag{14}$$

Which is the PI tracking law and the roots c_1 and c_2 are chosen such that both c_1 and c_2 are greater than zero. After finding ϑ, it is passed through a limiter to keep its value between ± 1.0 (maximum and minimum value of a cosine function). Fig. 4 shows the feedback linearising controller for the HVDC link. The values of K_1, K_2 and K_3 are constrained to the values as K_1, $K_2 > 0$, and $K_3 < 0$. This implements the solution of the Eqs. (9)–(14) in a block diagram fashion to obtain the firing angle o the rectifier.To estimate the parameters K_1, K_2 and K_3 a neural estimator in the form of an adaline is used. The inputs to the adaline are grouped in a vector form as

$$X = [\cos\alpha_r \quad \cos\alpha_i \quad I_{dc}]^T \tag{15}$$

and, T, transpose of a quantity. The output of the neural estimator is $\dot{I}_{dc}$.

3.1. Neural estimation algorithm

A generalized weight adaptation algorithm for the adaptive linear combiner is used to identify the parameters K_1, K_2 and K_3 of the HVDC link. In this algorithm, the learning parameters are adjusted to force the error between the actual and desired signal to satisfy a stable
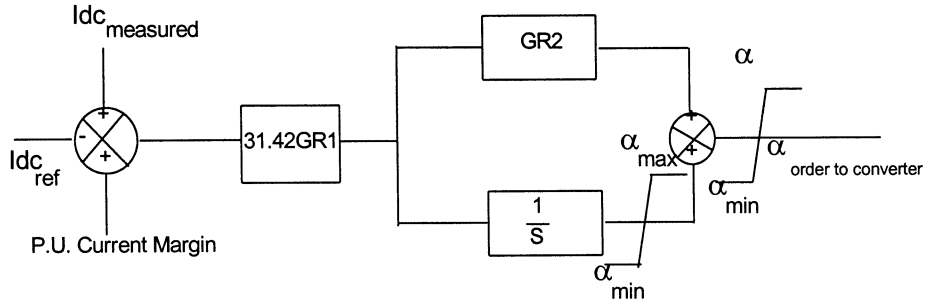
Fig. 3. Inverter pole controller.

difference error equation, rather than minimizing the error function. This approach allows one to better control the stability and speed of convergence by appropriate choice of the nonlinear function and learning parameters.

The basic equation of the neural estimator is

$$\hat{y} = WX \tag{16}$$

where $\hat{y}$ is the estimated value of the $\dot{I}_{dc}$, X is the input vector, W is the weight vector.

The weight vector of the adaline is updated using the Widrow–Hoff delta rule as

$$W(i+1) = W(i) + \frac{\alpha e(i)\theta(X_i)}{\lambda + X_i^T \theta(X_i)} \tag{17}$$

where,

$$\theta(X_i) = SGN(X_i) \tag{18}$$

$$SGN(x_i) = 1 \quad \text{if} \quad x_i > 0 \tag{19}$$

$$SGN(x_i) = -1 \quad \text{if} \quad x_i < 0$$

$$SGN(x_i) = 0 \quad \text{if} \quad x_i = 0$$

where i, time index; α, learning parameter; λ, a small value to avoid computational blow off during zero input conditions;

$$e(i) = y(i) - \hat{y}(i)$$

is the error at the time i; $y(i)$ is the actual value of DC link current derivative $\dot{I}_{dc}$ at time i.

For a bounded input vector, the neural estimator satisfies the following properties:

(i) $\|W_i - W_0\| \le \|W_{i-1} - W_0\| \le \|W_{\text{initial}} - W_0\| \quad i$

$$> 1 \tag{20}$$

(ii) $\displaystyle\lim_{i \to \infty} \frac{e^2(i)}{\lambda + X_i^T \theta(X_i)} \to 0 \tag{21}$

where W_0 is the weight vector that corresponds to perfect learning of the dc link parameters K_1, K_2 and K_3. Further, it can be proved that if the learning

parameter α lies between 0 and 2, and $\lambda > 0$, the following inequality results:

$$\left[-2 + \frac{\alpha \theta^T(X_i)\theta(X_i)}{\lambda + X_i^T \theta(X_i)}\right] < 0 \tag{22}$$

and $\|W_i - W_0\|^2$ is a bounded non-increasing function and the error $e(i)$ will converge asymptotically to zero. After the weight vector converges to a steady value W_0, the parameters K_1, K_2 and K_3 are $K_1 = W_0$ (1), $K_2 = W_0$ (2) and $K_3 = W_0$ (3).

For training the neural estimator, the dc link is operated with conventional control at either ends. The current order to the rectifier pole controller is subjected to change very slowly but sinusoidally between $\pm 50\%$ of the set value. This makes the system operating point change dynamically with the controller setting. The adaline output has to follow this, making the weights converge globally to optimum values. After the training, a plot of the weights with respect to time is obtained to find out the average value. For implementing the integrated feedback linearising and neural controller, one needs to import the value of α_i from the inverter side or design an observer for estimating the inverter firing angle. This is possible by the same communication link that is used for current order transmission.

4. Procedure

The measured DC link current is passed through an integrator and differentiator separately to obtain the integral and derivative signals. The control ϑ is obtained by premultiplying the different gains with the derived signal and adding them in a summer (Figs. 4 and 5). A hard limiter limits the value of ϑ to ± 1.0. The inverse function block then calculates the value of α_r in radians. Again it is passed through another limiter to keep the firing angle within $\alpha_{\min}$ and $\alpha_{\max}$. The parameters(K_1, K_2, K_3) for the inverse function block are derived from the already trained adaline (Fig. 6).
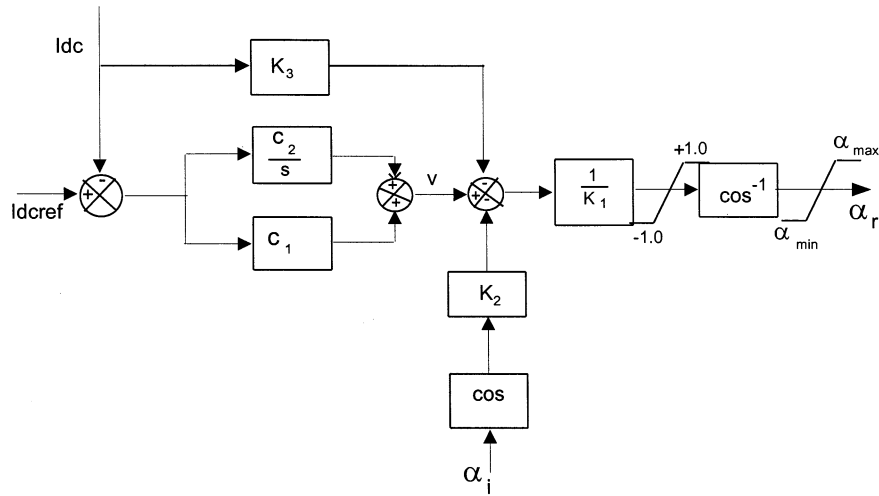
Fig. 4. Rectifier pole controller.

5. Case studied

To evaluate the effectiveness of this approach the DC link is subjected to the following transient conditions. The relevant waveforms demonstrate the feasibility as well as superiority of the proposed controller [6–10]. The following parameters are used for the controllers on either side. Rectifier Pole Controller: (Eq. (4), Fig. 5) $C1 = 700.0; C2 = 1.0; \alpha_{max} = 2.7$ rad.; $\alpha_{min} = 0.0873$ rad.; Rectifier Gamma Controller: (Fig. 2) $GP = 0.27; GI = 15.0; \alpha_{max} = 2.7$ rad.; $\alpha_{min} = 0.0873$ rad.; Inverter Pole Controller: (Fig. 3) $GR1 = 5.88; GR2 = 0.0136; \alpha_{max} = 3.14$ rad.; $\alpha_{min} = 1.9$ rad.; Inverter Gamma Controller: (Fig. 2) $GP = 0.27; GI = 15.0; \alpha_{max} = 3.14$ rad.; $\alpha_{min} = 1.9$ rad.

5.1. Single line-to-ground fault at the rectifier AC bus

A five-cycle single-line-to-ground fault has been created on the rectifier AC bus. The current and voltage waveforms are shown in Fig. 7. The DC current waveform resulting from the Linearising Control exhibits less oscillations (less overshoot and smaller settling time).
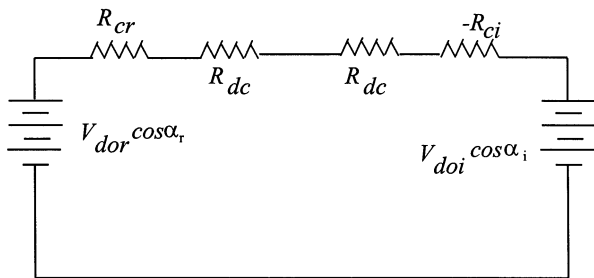
5.2. DC line-to-line-fault at the rectifier DC bus

A DC line-to-line fault has been created at the rectifier DC bus after the inductor for about five cycles. This is in a way similar to a three-phase fault on the AC bus as the net power flow becomes zero. The oscillations in case of the proposed controller are reduced drastically. The sudden dent in the current waveform is due to the dominating effect of integral action as the DC current error is positive throughout the fault. This sudden dent can be minimized by a proper selection of the gains. The relevant waveforms are shown in Fig. 8.

5.3. Single line-to-ground fault at inverter AC bus

The waveforms resulting from a five-cycle single line-to-ground fault at the inverter AC bus have been shown in Fig. 9. The current waveform in case of a conventional controller has a lot of crests and dents and suffers from prolonged oscillations, whereas, for a simple linearising control the DC current returns to it's nominal value without much oscillations.
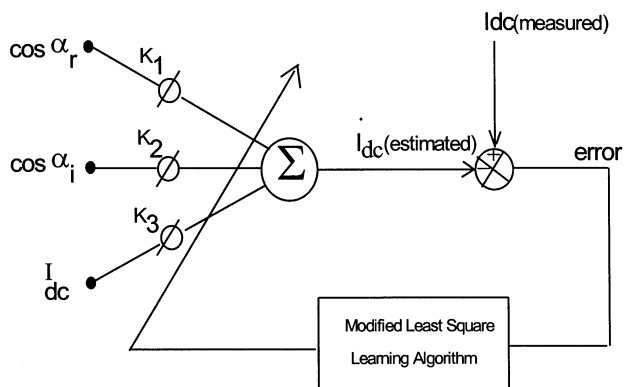

Fig. 5. Quasi steady state equivalent of DC link.
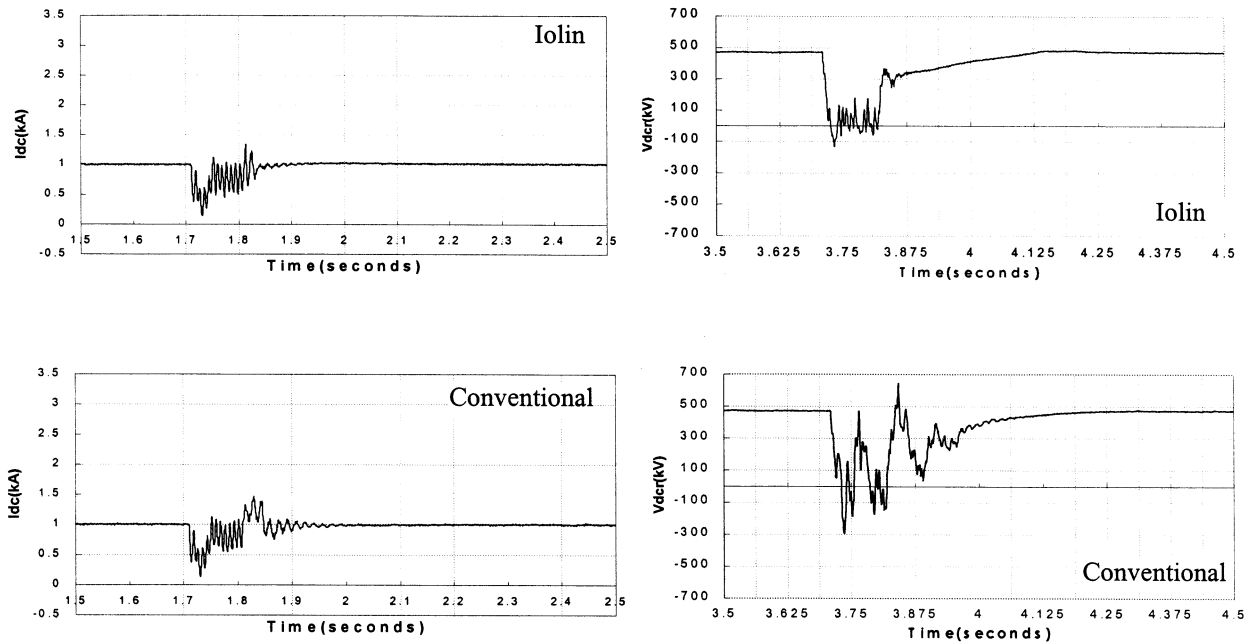

Fig. 6. The neural estimator.

Fig. 7. Single-line-to-ground fault on rectifier AC bus.

5.4. Single-line-to-ground fault at inverter AC bus with simultaneous change in SCR

The parameters of the above said controller have been optimised for the nominal value of the inverter and rectifier end short circuit impedance of the AC systems. To test the sensitivity of the proposed controller to the parameter variation, the short circuit impedance of the inverter end AC system is changed to

a different value and a five-cycle single line to ground fault on the inverter AC bus has been created to test the performance.

The nominal value (the controller gains are optimised at this value) (Fig. 1) $L_1 = 0.00767$, $HL_2 = 0.002735$, $HR = 1.267 \, \Omega$ (Rectifier AC System SCR $= 22 < 81.8°$), $L_1 = 0.0443$, $HL_2 = 0.0277$, $HR = 14.2 \, \Omega$ (Inverter AC System SCR $= 3.25 < 78°$)
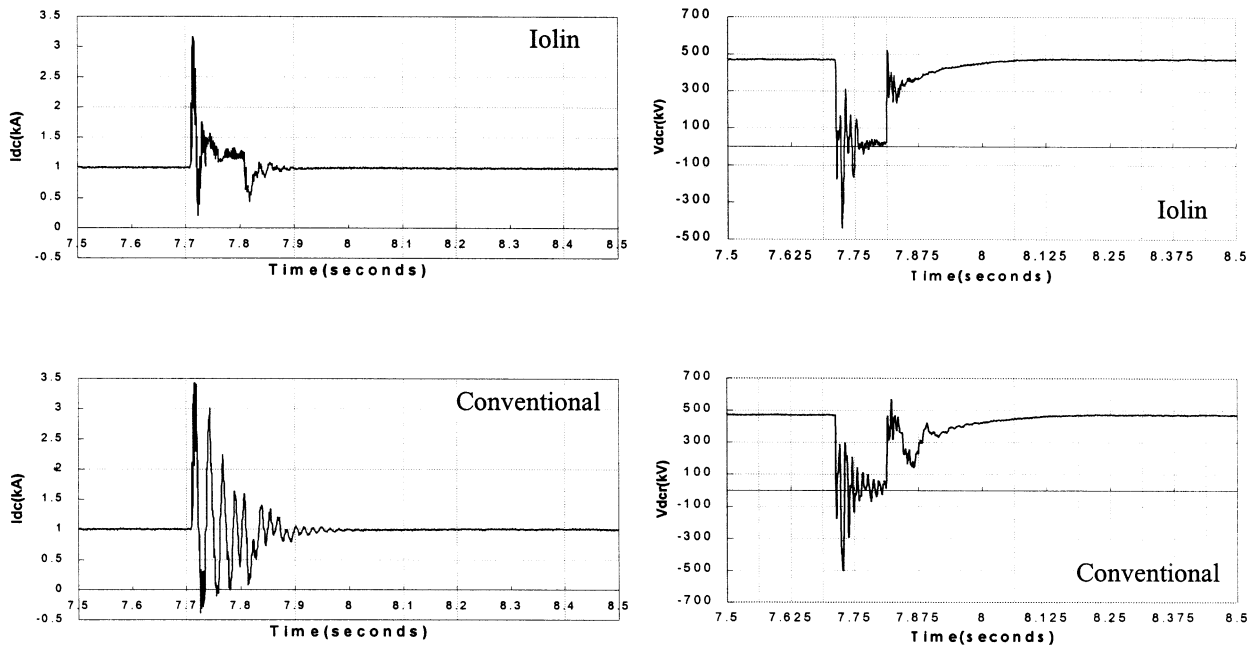
The changed value after the fault is cleared: $L_1 =$
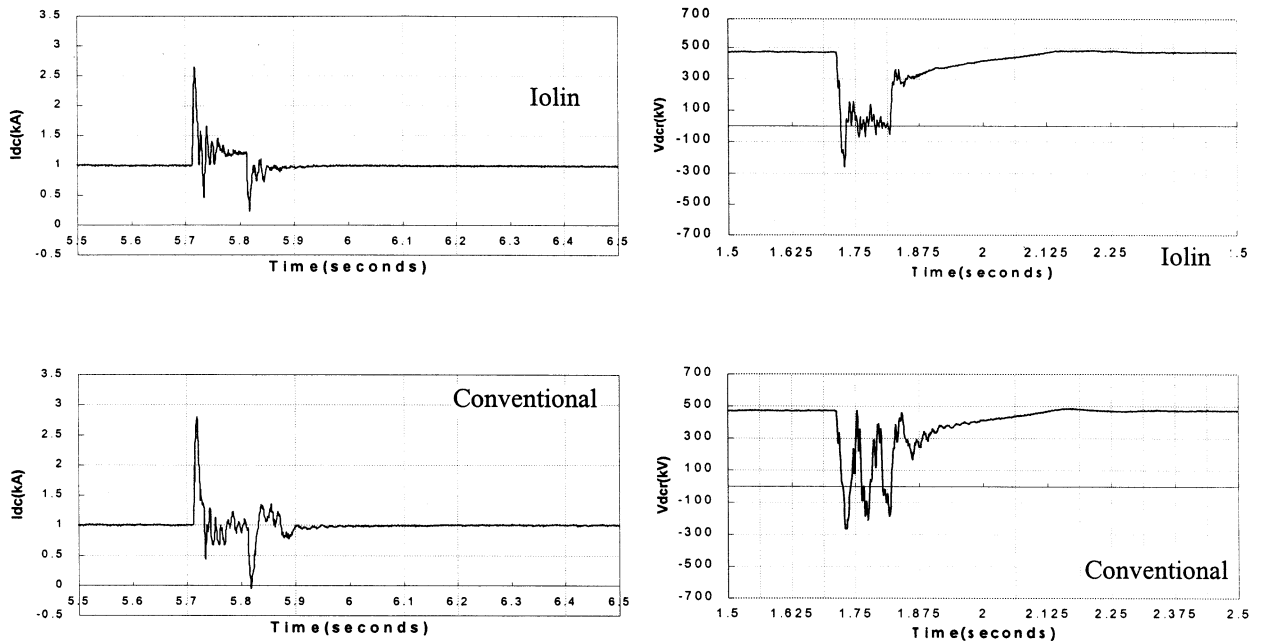

Fig. 8. DC-line-to-line fault at rectifier.

Fig. 9. Single-line-to-ground fault at inverter AC bus.

0.00767, $HL_2 = 0.02735$, $HR = 1.267$ Ω (Rectifier AC System SCR $= 22 < 81.8°$), $L_1 = 0.0443$, $HL_2 = 0.08$, $HR = 50.$ Ω (Inverter AC System SCR $= 1.9 < 71°$).Several commutation failures can be easily assessed from the oscillations in the Inverter DC voltage plots (Fig. 10). The comparative study from the voltage and current waveforms clearly shows the advantages of the proposed controller.

6. Discussions

From the above simulation results the following points are apparent.

1. In case of single-line-to-ground fault at rectifier AC bus the waveforms under the action of the proposed controller are not much improved over their conventional counterparts. However, in this case the
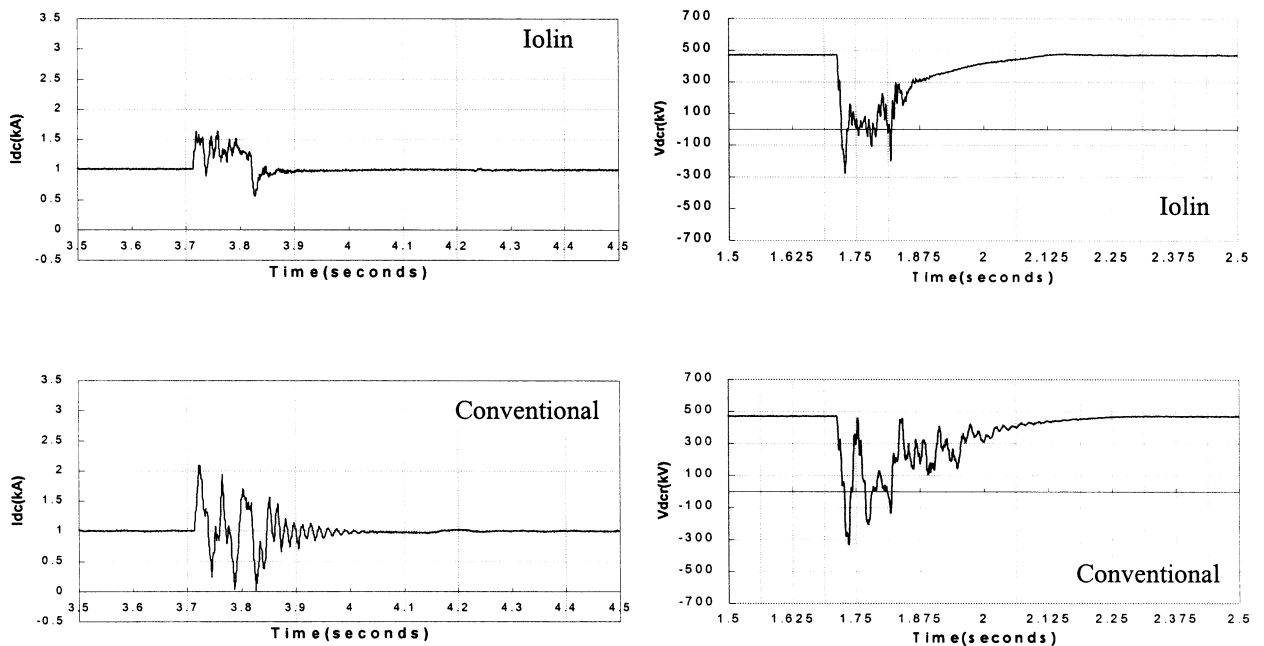

Fig. 10. Single-line-to-ground fault at inverter ac bus at a different value of SCR.

recovery is not as good as that under DC-line-to-ground fault. Such type fault gives rise to unbalanced operation of the converter where the ordinary DC link equations assumed for the controller do not hold good. Consequently one never gets the exact value of the firing angle where the converter should operate to keep the current at it's nominal value. As soon as the fault is cleared the DC link again returns to the balanced mode of operation and the controller is effective.

2. For DC-line-to-line fault at rectifier the oscillations in the DC link variables (voltage and current) are substantially smaller in comparison to those under conventional control. This is because of the fact that the AC side topology remains unchanged leading to the balanced operation of the converter. Thus the same linearising equations hold good here also. Therefore using it one gets back almost the exact value of the firing angle as soon as the fault is cleared. Only dent in the waveforms after the fault can be attributed to the saturation of the integrator used for tracking.

3. The waveforms resulting from the single-line-to-ground fault at inverter AC bus does not show appreciable improvement. Due to the unbalance created in the AC side the link no longer operates according to the assumed equations. Furthermore due to the low SCR the system transients do not die out fast. Therefore one never gets the exact firing angle that ought to be for the normal operation of the link. After the fault is cleared the link again recovers to the normal mode.

7. Conclusion

For HVDC transmission links, where very large transient conditions are involved in the plant operation, it is important to design control strategies, which are robust under all possible normal and abnormal situations. The above objective can be achieved only when there is a total knowledge of the system parameters. But for such systems where the AC subsystems are subjected to change their topology from time to time it is very difficult to have an accurate mathematical model. Also the non-linear nature of the link makes it difficult to design a time invariant robust controller for this sys-

tem. Feedback linearisation approach amounts to cancelling the non-linearities in a non-linear system so that the closed-loop dynamics is in a linear form. After developing the closed loop mathematical model the control action can be directly be expressed as any function of the error. Based on the above principle the results obtained display the superiority of such controllers over the conventional one. A little modification in the simple tracking law can make the controller performance better.

References

[1] S. Lefebvre, M. Saad, AR. Hurteau, Adaptive control for HVDC power transmission systems, IEEE Trans. Power Apparatus Syst. Vol. PAS-104, No.9, 1985, pp. 2329–2335.

[2] W.J. Rugh, Analytical framework for gain scheduling, IEEE Control Syst. Mag. II (1) (1991) 79–84.

[3] J. Reeve, M. Sultan, Gain scheduling adaptive control strategies for HVDC systems to accommodate large disturbances, IEEE Trans. Power Systfl. 9 (1) (1994) 366–372.

[4] Slotine, Wieping Li, Applied non-linear control, Prentice-Hall, Engelwood Cliffs, NJ, 1993.

[5] P.K. Dash, D.P. Swain, A.C. Liew, S. Rahman, An adaptive linear combiner for on-line tracking of power system harmonics, IEEE Trans. Power Syst. 11 (1) (1993) 37.

[6] K.W.V. To, A.K. David, A.E. Hammad, A robust co-ordinated control scheme for HVDC transmission with parallel AC systems, IEEE 94WM 061-2 PWRD.

[7] A.T. Alexandridis, G.D. Galanos, Design of an optimal current regulator for weak AC/DC systems using Kalman filtering in the presence of unknown inputs, IEE Proc. 136 (2) (1989) 57–63.

[8] S. Sood, N. Kandil, R.V. Patel, K. Khorasani, Comparative evaluation of neural network based and PI current controllers for HVDC transmission, IEEE Trans. Power Electron. 9 (3) (1994) 288–295.

[9] P.K. Dash, A.C. Liew, A. Routray, High performance controllers for HVDC links, Proc. IEE-Gen. Trans. Distrib. 141 (5) (1994) 422–428.

[10] A. Routray, P.K. Dash, A.C. Liew, A fuzzy self-tuning PI controller for HVDC links, IEEE Trans. Power Electron. 9 (2) (1994) 208–295.

[11] EMTDC User's Manual. Manitoba HVDC Research Center, Winnipeg, MB, Canada.